International Journal of Microwave and Wireless Technologies

cambridge.org/mrf

Research Paper

Cite this article: Shekhar S, Priya S, Kumar K (2024) A compact self-quintuplexing antenna by HM-SIW cavity. *International Journal of Microwave and Wireless Technologies*, 1–9. https://doi.org/10.1017/S1759078724001259

Received: 26 June 2024
Revised: 20 November 2024
Accepted: 22 November 2024

Keywords:
antenna; compact; half-mode substrate-integrated waveguide cavity; isolation; multiband operation; narrowband; one-eighth mode; pentaband; self-quintuplexing; triangular radiators

Corresponding author: Kundan Kumar;
Email: kundansingh.singh5@gmail.com

A compact self-quintuplexing antenna by HM-SIW cavity

Swapnil Shekhar[1], Shruti Priya[2] and Kundan Kumar[3]

[1]Department of Electronics and Communication Engineering, Sant Longowal Institute of Engineering and Technology, Sangrur, Punjab, India; [2]Department of Electronics Engineering, Indian Institute of Technology (ISM), Dhanbad, Jharkhand, India and [3]Department of Electronics and Communication Engineering, Dr. B. R. Ambedkar National Institute Technology, Jalandhar, Punjab, India

Abstract

This paper presents a novel compact self-quintuplexing antenna using a half-mode substrate-integrated waveguide cavity to implement multi-operation wireless services. The proposed antenna design incorporates five triangular protrusions of different dimensions, assembled with SIW to function as the radiating elements. Each radiator supports the one-eighth mode of the SIW cavity. The resonance frequencies of radiators are 3.63, 4.44, 5.23, 6.21, and 7.05 GHz. Each radiator operates at a distinct frequency due to the differing dimensions and is independently driven by 50 Ω microstrip lines. The measured reflection coefficients and isolation among any two ports are less than −10 dB and better than 23.6 dB, respectively. The measured gains at their respective resonant frequencies are 5.66, 4.84, 5.03, 7.08, and 6.59 dBi. The front-to-back ratio is better than 8.7 dB in each band. The difference of co-to-cross-polarization is greater than 19.3 dB.

Introduction

The meteoric rise in wireless communication technology and the proliferation of wireless devices have increased the demand for interoperable and functional systems [1]. Multiple antennas are needed to implement such a wireless system. Due to the use of multiple antennas, system size increases. A single port multiband antenna is used instead of multiple antennas to reduce the system size [1–3]. However, using a single port multiband antenna with a shared aperture restricts the operation of data transmission and reception simultaneously in a specific frequency band. An additional circuit, such as a multiplexer or filter, is required to separate the frequency band and provide adequate isolation among the frequency bands for easy selection of bands at the radio frequency (RF) front end to avoid intermodal inferences [4, 5]. The use of an additional circuit increases the overall system size and complexity. Therefore, several researchers around the globe are working on the development of a self-multiplexing antenna (SMA) using substrate integrated waveguide (SIW) to mitigate the challenges of wireless systems when a multiband antenna is used [6–17]. SMA operates simultaneously in multiple bands with independent ports for each band, providing adequate isolation between frequency bands without the use of additional circuits [6, 7]. shows the self-diplexing antennas, self-triplexing antennas are presented in references [8, 9], and [10–15] present the self-quadruplexing antennas. Very few self-quintuplexing antennas are available in the open literature [16, 17]. However, the self-quintuplexing antenna in references [16, 17] are designed using full mode SIW (FMSIW) cavity, which leads to an increase in size. Thus, designing a self-quintuplexing antenna in a compact size is challenging work.

This paper presents a novel compact self-quintuplexing antenna using a half-mode SIW cavity for pentaband wireless communication services. The proposed antenna comprises five different dimensioned triangular radiating elements in a circular half-mode SIW cavity. Each triangular radiating element radiates at distinct resonance frequencies of 3.63, 4.44, 5.23, 6.21, and 7.05 GHz, respectively. Each radiator supports the one-eighth mode of the SIW cavity. All frequency bands can be tuned independently. This antenna has at least an isolation of 23.6 dB among the ports and gains more than 4.84 dBi in all the bands.

Antenna configuration

The labeled diagram of the proposed self-quintuplexing antenna, with the top and exploded views, is shown in Fig. 1. Table 1 lists the values of the design parameters used to model the antenna. The proposed antenna is implemented on a 0.787 mm thick, single-layer Roger RT/Duroid 5880 substrate having a dielectric constant (ε_r) of 2.2 and a loss tangent (tan δ)

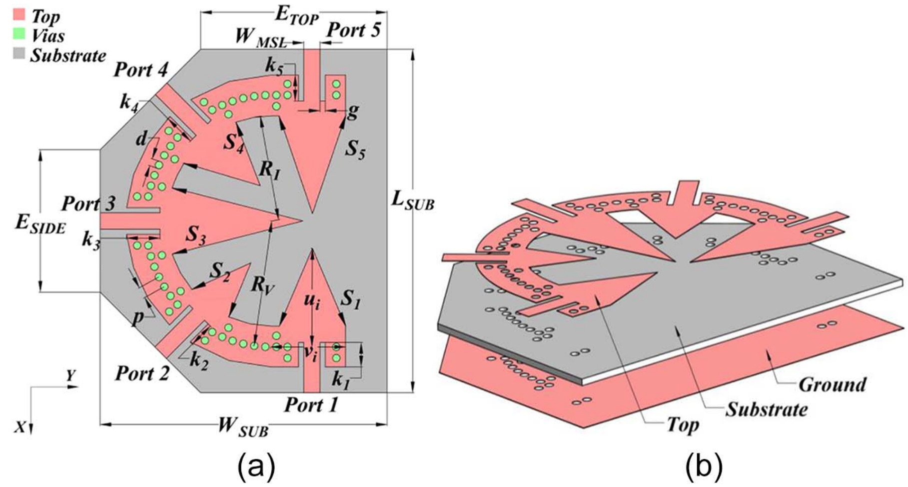

Figure 1. Labelled schematic diagram of the proposed self-quintuplexing antenna (a) Top view and (b) Exploded view.

Table 1. Value of design parameters used in schematic diagram

Param.	Value	Param.	Value	Param.	Value
S_1	22.84	u_1	13.3	L_{SUB}	46.41
S_2	16.6	u_2	10.49	W_{SUB}	38.95
S_3	36.46	u_3	20.54	E_{TOP}	25.22
S_4	19.9	u_4	11.68	E_{SIDE}	19.22
S_5	27.88	u_5	16	R_I	14.2
k_1	3.3	v_1	10.27	R_V	17.02
k_2	3.4	v_2	8.4	W_{MSL}	2.2
k_3	4.51	v_3	10.65	d	1
k_4	4.29	v_4	11.52	g	0.7
k_5	3.5	v_5	9.96	p	1.5

Param. stands for parameter; units: mm.

of 0.0009. The proposed design comprises five triangular protrusions of different dimensions that are assembled with the half-mode substrate-integrated waveguide (HM-SIW). Each triangular section acts as a radiating element and operates at distinct resonance frequencies of 3.63, 4.44, 5.23, 6.21, and 7.05 GHz, respectively. Each radiator supports the perturbed one-eighth mode of the SIW cavity and is individually fed by a 50 Ω inserted microstrip line. The antenna is optimized and analyzed using 3D electromagnetic (EM) software, Ansys's HFSS.

Antenna design and analysis

The proposed antenna is designed in an HM-SIW cavity, as shown in Fig. 1. A perturbed one-eighth mode of SIW cavity backs each radiator. Each radiator is created by dividing the FMSIW circular cavity resonator into eight parts along the lines AA', BB', CC', and DD', as shown in Fig. 2(a). One-eighth section of the FMSIW resonator is shown in Fig. 2(b). A geometry of the individual triangular radiating element backed by the eighth-mode SIW resonator is depicted in Fig. 2(c). Each eighth-mode SIW resonator is excited by a 50 Ω inserted microstrip feedline. The proposed resonator works in the fundamental TE_{110} mode. The resonant frequency of each radiator can be calculated by (1) [18]

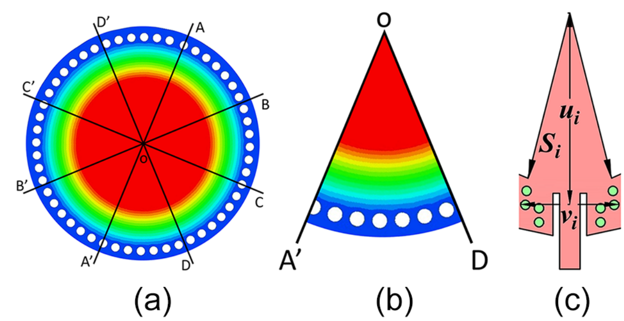

Figure 2. Electric field distribution in (a) SIW full cavity, (b) One-eighth mode cavity, and (c) Geometry of a single triangular radiating element backed by an eighth mode of SIW cavity resonator.

$$f_{mn0} = \frac{1.8412}{2\pi\sqrt{\mu\varepsilon}\, u_i} \tag{1}$$

where $u_{i(i\,=\,1,2,3,4,\ and\ 5)}$ is the dimension of the i^{th} port radiator; ε and μ are the permittivity and permeability of the substrate. The resonance frequency of some radiators is shifted from the calculated resonance frequency (1) due to the loading effect. Thus, equation (1) is used as an initial design rule for the calculation and selection of dimensions at a given operating frequency. The five radiating elements with unique dimensions are placed in the HM-SIW cavity to enable the operation at different operating frequencies. To maintain the sufficient gap between the radiators, the use of differently dimensioned radiators, and the placement of vias according to the design rule (2) [19]

$$p < 2.5d \tag{2}$$

where p is the longitudinal spacing between two vias, also known as the pitch and d is the diameter of the via; ensures adequate isolation between the radiators by preventing spreading of radiation leakage, thus increasing the isolation.

E-field distribution

Figure 3 depicts the magnitude distributions of the electric fields in the proposed antenna structure after applying excitation at each port independently. The magnitude of the electric field is maximum at the respective triangular radiator when excited independently and almost zero at other triangular radiators, as shown

https://doi.org/10.1017/S1759078724001259 Published online by Cambridge University Press

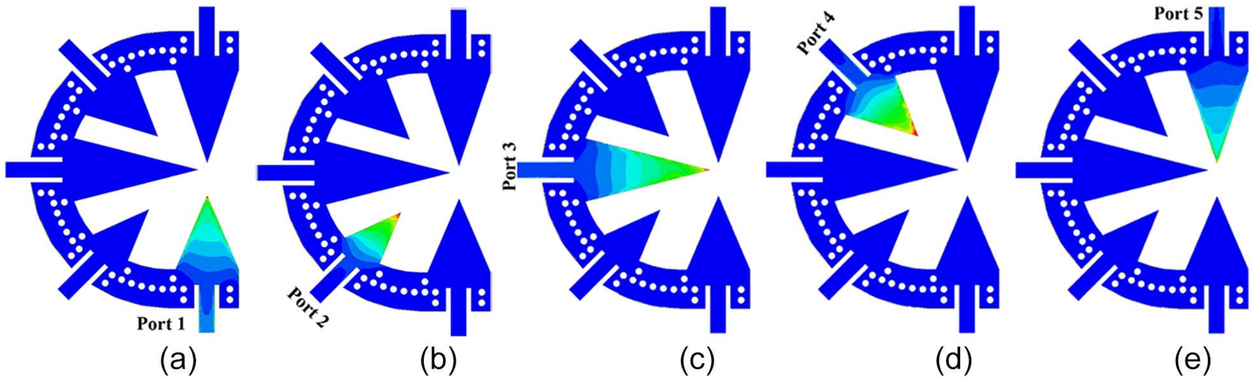

Figure 3. Magnitude of electric-field distribution when power is fed from respective port (a) Port 1, (b) Port 2, (c) Port 3, (d) Port 4, and (e) Port 5.

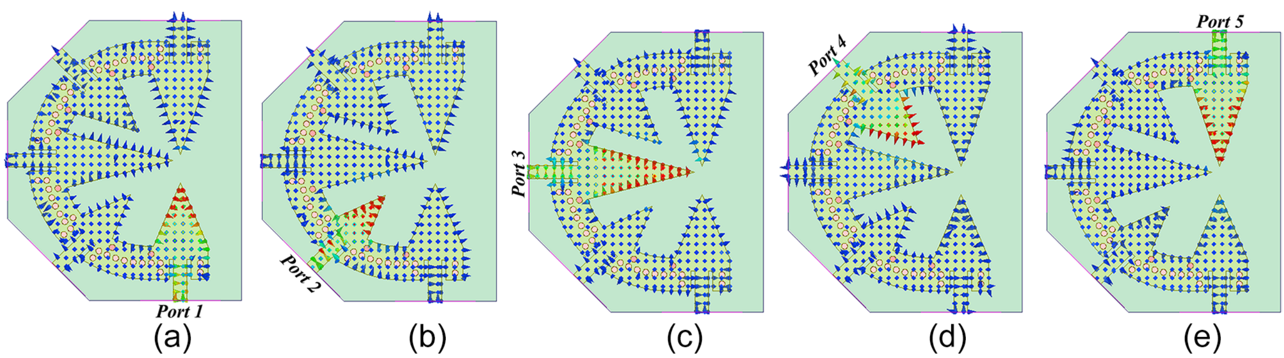

Figure 4. Vector electric-field distribution when power is fed from respective port (a) Port 1, (b) Port 2, (c) Port 3, (d) Port 4, and (e) Port 5.

in Fig. 3(a–e). This figure shows that the radiation occurs from the open edge of the triangular protrusions. The distributions of the vector electric fields in the proposed antenna structure after applying excitation at each port independently are shown in Fig. 4(a–e). The vector electric field distribution shows radiation occurs due to the fringing field present at the edges of the triangular protrusions. The electric field distribution also confirms that each radiator supports the perturbed one-eighth mode of TE_{110} mode.

Equivalent circuit model

The equivalent circuit model acts as a reference to simulate the antenna's interaction with the system. The corresponding circuit model of the proposed self-quintuplexing antenna circuit using lumped elements is shown in Fig. 5(a). Each one-eighth cavity resonator can be represented by a parallel resistor (R), inductor (L), and Capacitor (C) (RLC) tank circuit. In Fig. 5(a), R_{Ai}, C_{Ai}, and L_{Ai} are the equivalent resistance, capacitance, and inductance associated with the individual ports, and i represents the port number from 1 to 5. The gap between the radiators acts as a shunt capacitor (C_{Si}). M_{ij} represents the mutual coupling between two ports, i and j, where i, j can assume values from 1 to 5 and $i \neq j$. A series LC circuit represents the analogous circuit architecture for mutual coupling between any two radiators, where L_{Mij} and C_{Mij} symbolize inductance and capacitance, respectively. The resonant frequency of the resonators is calculated by (3) [20]

$$f_{0i} = \frac{1}{2\pi\sqrt{L_{Ai}C_{Si}}} \tag{3}$$

Table 2. Value of components of the circuit model

Comp.	Value	Comp.	Value	Comp.	Value
R_{A1}	259	L_{A1}	0.17187	C_{A1}	0.6008094
R_{A2}	316.5	L_{A2}	0.10893	C_{A2}	0.94688
R_{A3}	414.25	L_{A3}	0.1459	C_{A3}	0.93191
R_{A4}	217	L_{A4}	0.1079	C_{A4}	0.67292
R_{A5}	169.25	L_{A5}	0.09096	C_{A5}	0.39696
C_{S1}	5.057072	$L_{M2,1}$	7	$C_{M2,1}$	10.7
C_{S2}	3.964	$L_{M3,1}$	19.50087	$C_{M3,1}$	24.00084
C_{S3}	12.961	$L_{M4,1}$	16	$C_{M4,1}$	12
C_{S4}	5.623	$L_{M5,1}$	20	$C_{M5,1}$	15.0009
C_{S5}	14.055	$L_{M3,1}$	6	$C_{M3,2}$	12.4
$N1$	0.45	$L_{M4,2}$	10.29293	$C_{M4,2}$	11.5
$N2$	0.4	$L_{M5,2}$	18	$C_{M5,2}$	9
$N3$	0.35	$L_{M4,3}$	9	$C_{M4,3}$	11
$N4$	0.5	$L_{M5,3}$	14	$C_{M5,3}$	13
$N5$	0.55	$L_{M5,4}$	15	$C_{M5,4}$	9.92

Comp. stands for component; units: resistance = Ω, inductance = nH and capacitance = pF

The input impedance is calculated by (4)

$$Z_{in} = \frac{j\omega_{0i}L_{Ai}}{1 - \omega_{0i}^2 L_{Ai}C_{Si}} \tag{4}$$

https://doi.org/10.1017/S1759078724001259 Published online by Cambridge University Press

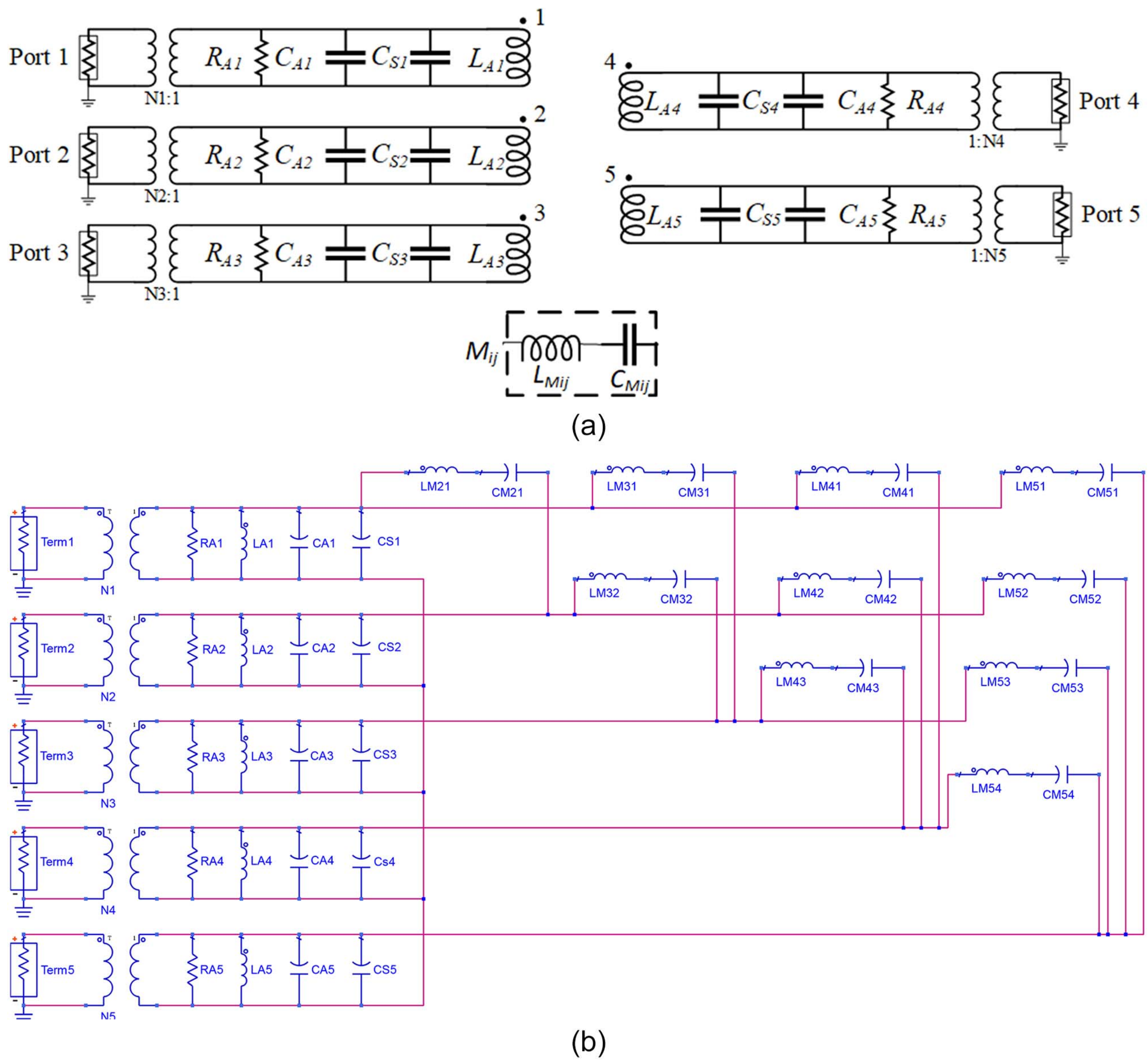

Figure 5. (a) Equivalent circuit model and (b) circuit design in Keysight ADS of proposed self-quintuplexing antenna.

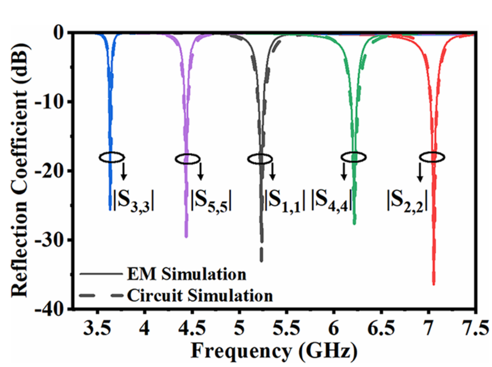

Figure 6. Comparison of reflection coefficient values of EM and circuit simulation of the proposed antenna.

The resonant frequency is related to the shunt capacitance C_{si} and inductance L_{Ai} as given in equation (3). By changing the dimensions of the radiator, the corresponding resonant frequency can be varied. The equivalent lumped circuit model is simulated and optimized using Keysight Advanced Design System (ADS). The schematic diagram of the circuit designed in ADS is shown in Fig. 5(b). Significant agreement exists between the EM simulated and circuit simulated reflection coefficient values, as shown in Fig. 6. Figure 7(a) and (b) illustrate the isolation values for EM simulation, while Fig. 7(c) and (d) show the isolation values for circuit simulation. The isolation values between any two ports are greater than 23.6 dB in both the simulations. The value of the circuit components obtained after optimization is given in Table 2.

https://doi.org/10.1017/S1759078724001259 Published online by Cambridge University Press

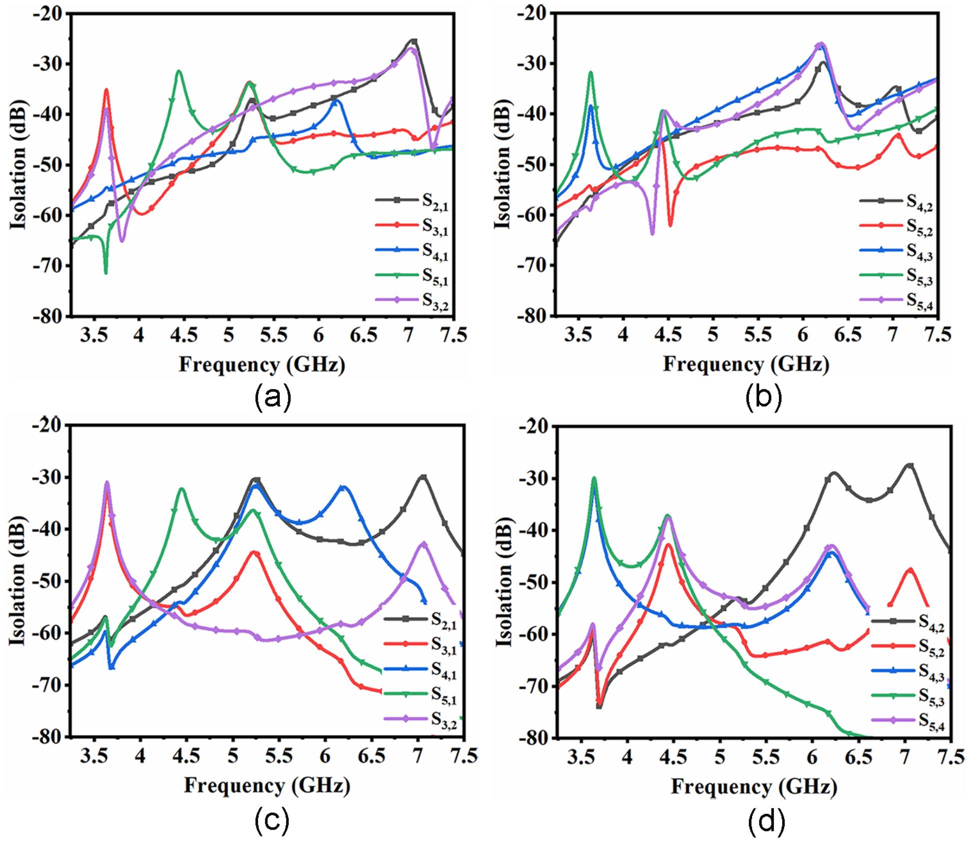

Figure 7. Isolation for (a and b) EM simulation and (c and d) circuit simulation of the proposed antenna.

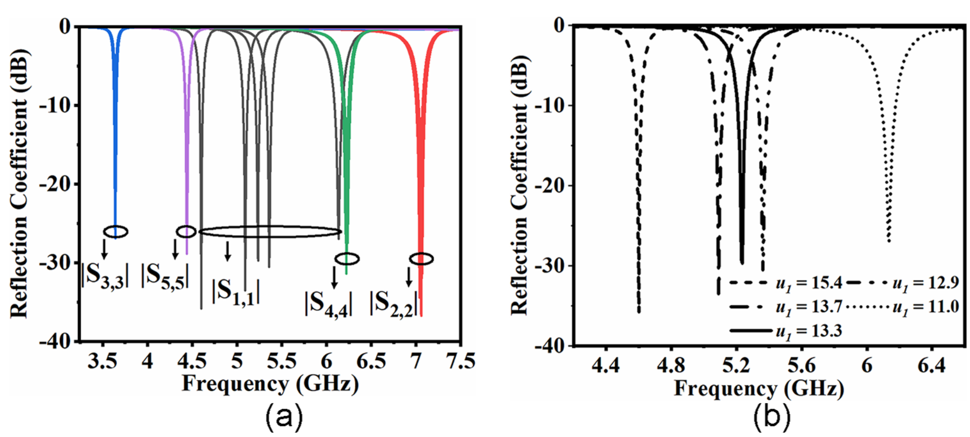

Figure 8. Variation in reflection coefficient with u_i (units: mm) keeping other dimensions constant (a) Port 1, (b) Magnified view of frequency variation.

Tuning of operating frequencies

The proposed antenna design allows independent tuning of each radiating element's operating frequency. The resonant frequency tuning is performed by changing the dimension $u_{i(i\,=\,1,2,3,4,\ and\ 5)}$ of the triangular radiating element, where i represents the port number. A parallel resonant circuit represents an unperturbed one-eighth mode cavity. As shown in the equivalent circuit model, a shunt capacitance represents the gap between radiators. When the length (u_i) of the triangular radiator decreases, the shunt capacitance also decreases. As the resonant frequency is inversely proportional to capacitance, thus the resonant frequency increases. Figure 8 shows the variation in the reflection coefficient at the resonant frequency due to a change in the dimension u_1 of the radiator at port 1. u_1 assumes the values 15.4, 13.7, 13.3, 12.9, and 11.0 mm. The highest resonant frequency (f = 6.13 GHz) is obtained at u_1 = 11.0 mm, and the lowest resonant frequency (f = 4.6 GHz) is obtained at u_1 = 15.4 mm. As frequency tuning is conducted without altering the initial cavity dimensions, there is no significant impact on other antenna performance characteristics. The

https://doi.org/10.1017/S1759078724001259 Published online by Cambridge University Press

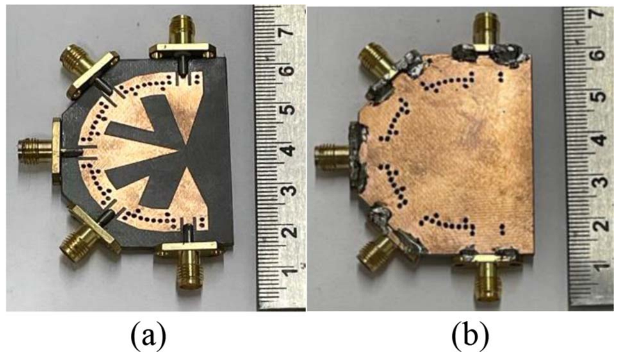

Figure 9. Image of fabricated antenna (a) Top and (b) Bottom.

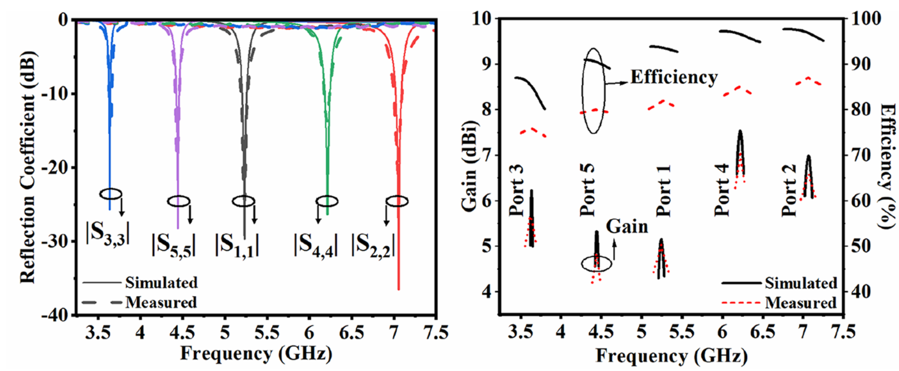

Figure 10. Simulated and measured (a) Reflection coefficient and (b) Gain and efficiency.

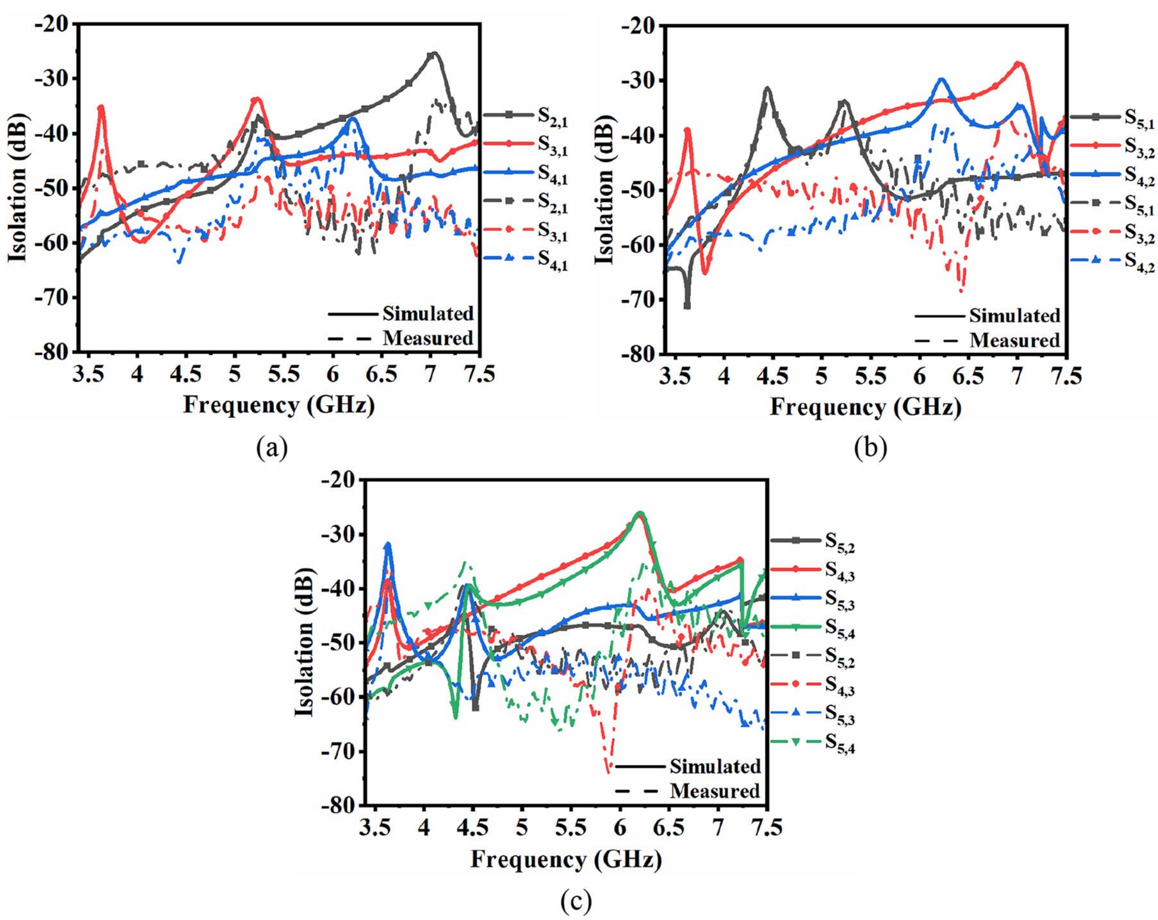

Figure 11. Simulated and measured isolation for the proposed antenna.

https://doi.org/10.1017/S1759078724001259 Published online by Cambridge University Press

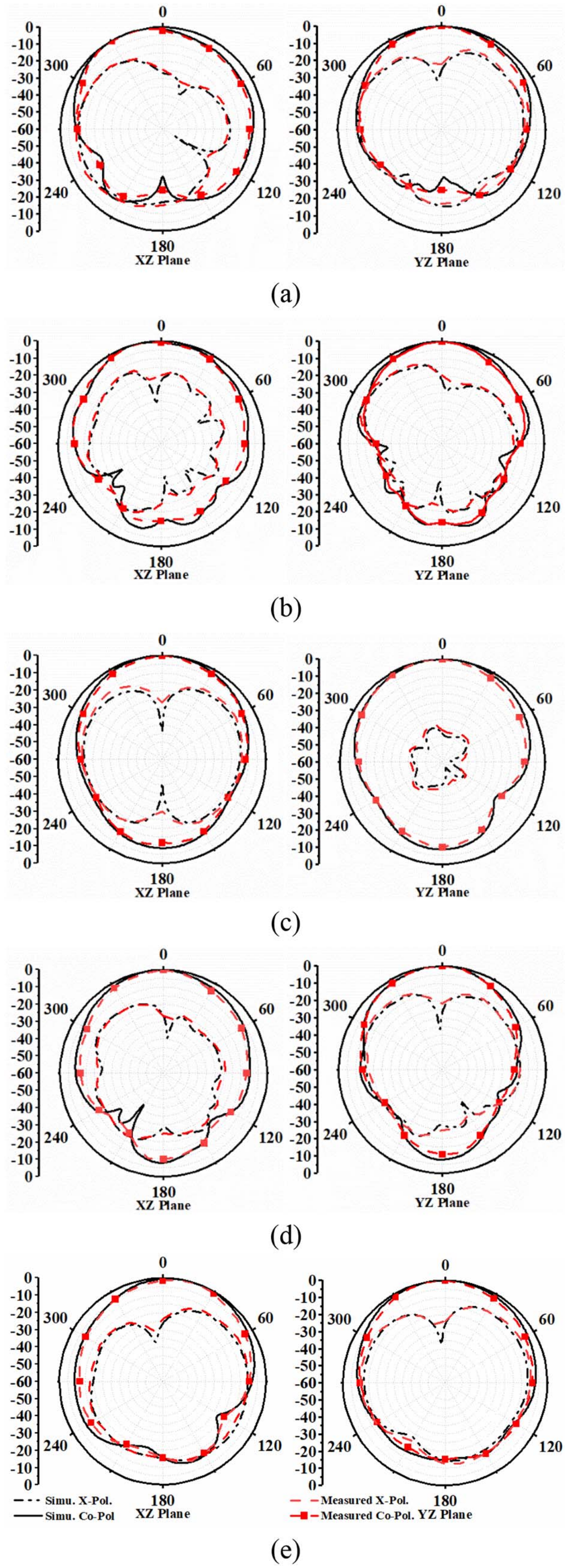

Figure 12. Simulated and measured radiation pattern at a frequency of (a) 5.23 GHz, (b) 7.05 GHz, (c) 3.63 GHz, (d) 6.21 GHz, and (e) 4.44 GHz.

Table 3. Result of measured antenna parameters

Port excited	Resonant frequency (GHz)	Minimum isolation (dB)	Gain (dBi)	Cross polarization (dB)	Front-to-back ratio (dB)
1	5.23	23.6	5.03	22.02	13.06
2	7.05	30.3	6.59	19.30	11.81
3	3.63	24.5	5.66	26.97	8.73
4	6.21	24.5	7.08	26.82	8.89
5	4.44	23.6	4.84	22.75	14.17

proposed antenna design can be operated at any desired frequency between 3 and 8.3 GHz by varying the length (u_i) of the triangular radiators. The 10 dB fractional bandwidth (%) of the radiator varies from 0.36% (10.9 MHz) to 1.41% (89.6 MHz). Minimum separation among any two frequencies is kept 80 MHz to maintain at least 20 dB isolation. In the band tuning of any radiator, the simulated isolation is maintained better than 20 dB. The following design steps are suggested based on the above study:

1) Select the radius of the circular cavity $R_V \approx 0.14\ \lambda_g$, where $\lambda_g = \lambda_0/\sqrt{\varepsilon_r}$ is the guided wavelength at the lowest mid-band frequency.
2) Model the radiator, with its radiating edge length S_i of $\lambda_g/2$, and the vertex should be at $\lambda_g/4$ from the respective port.
3) Optimize each port for $|S_{11}| < -15$ dB by modifying the length of the respective inset.
4) Adjust the length (u_i) or base (v_i) of the radiator to attain the preferred resonant frequency.
5) Repeat steps (3) and (4) until the desired results are obtained for each slot.

Result and discussion

A self-quintuplexing antenna using an HM-SIW cavity is fabricated on a single layer Roger RT/Duroid 5880 substrate to validate the antenna. Figure 9 shows the fabricated antenna. Figure 10(a) depicts the simulated and measured reflection coefficients of the proposed antenna. The matching of the measured reflection coefficient of all ports is less than −20 dB. Figure 10(b) illustrates the simulated and measured antenna gain and efficiencies which are more than 4.84 dBi and 76%, respectively. The measured isolation between any two ports is better than 23.6 dB, as shown in Fig. 11. Figure 12 illustrates the radiation patterns for each port. The measured front-to-back ratio (FTBR) and co-to-cross polarization are more than 8.7 and 19.3 dB in all bands. Table 3 presents the measured antenna parameters. Table 4 compares performance parameters between the proposed and previous work. The size of the proposed antenna is smaller than all the antennas presented except [14], whereas antennas [10–15] are self-quadruplexing antennas. The proposed antenna is suitable for RF front end system of various use cases and practical applications such as 5G NR, Wi-Fi, C-band communication satellite, and other narrowband applications in 3–8.3 GHz.

https://doi.org/10.1017/S1759078724001259 Published online by Cambridge University Press

Table 4. Comparison of the proposed self-quintuplexing antenna with other self-multiplexing SIW antenna designs

Ref.	Resonant frequencies (GHz)	Minimum isolation (dB)	Gain (dBi)	10 dB fractional bandwidth (%)	FTBR (dB)	Size (λ_g^2)
[10]	8.19/8.78/9.71/11	>22	5.5/6.9/7.47/7.45	2.07/1.93/2.78/2.81	>17	0.94
[11]	8.85/10.4/11.4/12.23	>26	5.4/6.4/6.8/6.7	2.71/3.55/4.64/5.23	>15	1.87
[12]	3.5/4.9/5.4/5.8	>23.1	4.4/5.07/5.4/5.7	2.2/3.05/3.14/3.2	>16.5	0.32
[13]	2.45/3.5/4.9/5.4	>29.9	3.85/5.33/5.95/5.97	4.69/5.14/4.08/4.1	NR	0.23
[14]	2.33/2.96/5.43/6.15	>32.5	4.21/3.39/6.1/4.34	1.28/0.85/1.38/1.3	NR	0.125
[15]	5.8/7.4/28/38	>26	4.1/5.2/6.1/8.3	1.72/1.35/1.42/1.57	NR	0.25
[16]	5.2/5.5/5.8/6.2/6.8	>20	5.2/6.8/5.1/4.6/4.2	NR	>14.2	0.28
[17]	2.29/2.98/3.65/4.37/5.08	>29.31	3.59/4.55/3.91/5.70/4.92	0.41/0.67/0.73/0.99/1.15	NR	0.23
This work	**3.63/4.44/5.23/6.21/7.05**	**>23.6**	**5.66/4.84/5.03/7.08/6.59**	**0.86/1.0/1.47/1.05/1.41**	**>8.7**	**0.186**

NR: not reported; FTBR: front-to-back ratio

Conclusion

This paper presents a novel self-quintuplexing antenna using an HM-SIW cavity for pentaband wireless communication services. The five frequency bands can be tuned independently to operate at the required center frequency according to the intended functionality. The antenna has high gain and isolation, better than 4.84 dBi and 23.6 dB, respectively. It has co-to-cross polarization that is better than 19.3 dB. The size of the proposed antenna is smaller than most of the antennas presented in Table 4. The measured performance parameters demonstrate the effectiveness of the proposed antenna for possible application in systems with support for multiple communication standards.

Acknowledgements. We would like to thanks the Science and Engineering Research Board (SERB), DST, Govt. of India, for providing basic infrastructure for this work under the sanctioned project number SRG/2022/000664. We would also like to thank Dr. B. R. Ambedkar NIT Jalandhar, for providing fabrication facility under the sanctioned project number NITJ/DRC/4710.

Competing interests. The authors report no competing interests.

References

1. **Alsath MGN and Kanagasabai M** (2013) Planar pentaband antenna for vehicular communication application. *IEEE Antennas and Wireless Propagation Letters* **13**, 110–113.
2. **Wang H, Liu X, Fang Z, Zhang R and Wang Y** (2023) Penta-band rectangular slot antenna for multi-function wireless communication with linear and circular polarizations. *International Journal of Microwave and Wireless Technologies* **15**, 1382–1391.
3. **Hu W, Yin Y-Z, Yang X and Fei P** (2013) Compact multiresonator-loaded planar antenna for multiband operation. *IEEE Transactions on Antennas and Propagation* **61**, 2838–2841.
4. **Liu H, Xu W, Zhang Z and Guan X** (2013) Compact diplexer using slotline stepped impedance resonator. *IEEE Microwave and Wireless Components Letters* **23**, 75–77.
5. **Wei F, Liu W-S, Wang JX and Zhao X-B** (2022) Design of a novel balanced-to-balanced dual-band diplexing power divider. *IEEE Transactions on Circuits and Systems II: Express Briefs* **70**, 516–520
6. **Priya S, Kumar K and Mandal MK** (2020) Circularly polarized self-diplexing SIW cavity-backed slot antenna. *IEEE Transactions on Antennas and Propagation* **68**, 2387–2392.
7. **Iqbal A, Al-Hasan M, Mabrouk IB and Nedil M** (2021) Ultracompact quarter-mode substrate integrated waveguide self-diplexing antenna. *IEEE Antennas and Wireless Propagation Letters* **20**, 1269–1273.
8. **Kumar K and Dwari S** (2017) Substrate integrated waveguide cavity-backed self-triplexing slot antenna. *IEEE Antennas and Wireless Propagation Letters* **16**, 3249–3252.
9. **Priya S and Dwari S** (2020) A compact self-triplexing antenna using HMSIW cavity. *IEEE Antennas and Wireless Propagation Letters* **19**, 861–865.
10. **Priya S, Kumar K and Mandal MK** (2019) Compact self-quadruplexing SIW cavity-backed slot antenna. *IEEE Transactions on Antennas and Propagation* **67**, 6656–6660.
11. **Kumar SP, Dwari S and Mandal MK** (2020) Self-quadruplexing circularly polarized SIW cavity-backed slot antennas. *IEEE Transactions on Antennas and Propagation* **68**(8), 6419–6423.
12. **Iqbal A, Mabrouk IB and Nedil M** (2020) Compact SIW-based self-quadruplexing antenna for wearable transceivers. *IEEE Antennas and Wireless Propagation Letters* **20**, 118–122.
13. **Iqbal A, Tiang JJ, Wong SK and Mallat NK** (2021) SIW cavity-backed self-quadruplexing antenna for compact RF front ends. *IEEE Antennas and Wireless Propagation Letters* **20**, 562–566.
14. **Barik RK and Koziel S** (2022) Highly miniaturized self-quadruplexing antenna based on substrate-integrated rectangular cavity. *IEEE Antennas and Wireless Propagation Letters* **22**, 482–486.
15. **Pour Mohammadi P, Naseri H, Melouki N, Ahmed F, Iqbal A, Vandenbosch GA and Denidni TA** (2023) Compact SIW-based self-quadruplexing antenna for microwave and mm-wave communications. *IEEE Transactions on Circuits and Systems II: Express Briefs* **70**, 3368–3372.
16. **Chaturvedi D, Kumar A, Althuwayb AA and Ahmadfard F** (2023) SIW-backed multiplexing slot antenna for multiple wireless system integration. *Electronics Letters* **59**, e12826.
17. **Barik RK and Koziel S** (2023) Design of compact self-quintuplexing antenna with high-isolation for penta-band applications. *IEEE Access* **11**, 30899–30907.
18. **Pozer DM** (1998) *Microwave Engineering*. New York, NY: Wiley.
19. **Xu F and Wu K** (2005) Guided-wave and leakage characteristics of substrate integrated waveguide. *IEEE Transactions on Microwave Theory & Techniques* **53**, 66–73.
20. **Marcuvitz N** (1951) *Waveguide Handbook*. Edison, NJ: IET.

Swapnil Shekhar received his B. E. degree in Electronics and Communication Engineering from Thapar Institute of Engineering and Technology, Patiala, India, in 2019 and received his M. Tech. degree from Sant Longowal Institute of Engineering and Technology, Sangrur, India, in 2023. He is currently pursuing his Ph.D. degree from the Department of Electrical Engineering, Indian Institute of Technology, Delhi, India. His research interests include development of novel antenna, substrate-integrated waveguide, smart sensors, and their integration.

Dr. Shruti Priya received her B. Tech in Electronics and CommunicationEngineering in 2012 from Dr. M. G. REducational and Research Institute, Chennai, India, M. Tech in Digital Communication in 2015 from RGPV, Bhopal, India and PhD from Indian Institute of Techonology (ISM) Dhanbad, India. She worked as a post doctorial fellow and Research Associate at Institute for Plasam Research, Gandhinagar, India and Indian Institute of Techonology Mandi, India respectively. Shruti Priya has published several research papers in referred International Journals and Conferences. Her research interest in substrate integrated waveguide based antennas, multiband antennas, and self-multiplexing antennas.

Dr. Kundan Kumar received his B. Tech in Electronics and Communication Engineering in 2012, M. Tech and Ph.D. in Electronics and Communication Engineering from Indian Institute of Technology (ISM), Dhanbad, Jharkhand, India in year 2015 and 2020 respectively. Dr. Kumar working as Assistant Professor in the Department of Electronics and Communication Engineering at Dr. B R Ambedkar National Institute of Technology Jalandhar, Punjab, India. Prior to this, he worked as Assistant Professor in the Department of Electronics and Communication Engineering at PEC Chandigarh and SLIET Longowal Respectively. Dr. Kumar was continuously qualified seven times Graduate Aptitude Test in Engineering in the subject of Electronics and Communication Engineering and top 0.76% students in 2013. He was also continuously two times qualified National Eligibility Test for Assistant Professor in the subject of Electronic Science under University Grants Commission in June-2014 and December-2014. Dr. Kumar received the Research Publication Award by IIT Dhanbad in the year of 2017 and Research Project Award by SLIET Longowal in the year of 2023. Dr. Kumar has published 20 research papers in referred International Journals (like IEEE Transactions on Antennas and Propagation, IEEE Antennas and Wireless Propagation Letters and etc.) and Conferences. Dr. Kumar delivered expert talk in several institute.He is a regular reviewer of various referred International Journals like IEEE Transactions on Antennas and Propagation, IEEE Antennas and Wireless Propagation Letters and etc. His research interest includes 5G antennas and circuits, RF and millimeter wave antennas, intelligent antennas for cognitive radio, characterization of dielectric material, modelling and analysis substrate-integrated waveguide-based antennas, self-multiplexing antennas, RF planar circuits, RF/microwave sensors and computational electromagnetics.

https://doi.org/10.1017/S1759078724001259 Published online by Cambridge University Press